Chapter 3

Allosteric Coupling Between Transition Metal-Binding Sites in Homooligomeric Metal Sensor Proteins

Nicholas E. Grossoehme and David P. Giedroc

Abstract

Intracellular concentrations of transition metal ions are controlled at the transcriptional level by a panel of metalloregulatory proteins that collectively allow the cell to respond to changes in bioavailable metal concentration to elicit the appropriate cellular response, e.g., upregulation of genes coding for metal export or detoxification proteins in the event of metal excess. These proteins represent a specialized class of allosteric regulators that are ideal for studying ligand-mediated allostery in a comprehensive way due to the size, stability, reactivity, and the spectroscopic properties of transition metal ions as allosteric ligands. In addition to the commonly studied heterotropic regulation of metal binding and DNA binding, many of these proteins exhibit homotropic allostery, i.e., communication between two or more identical metal (ligand) binding sites on an oligomer. This chapter aims to guide the reader through the design and execution of experiments that allow quantification of the thermodynamic driving forces (ΔG_C, ΔH_C, and ΔS_C) that govern both homotropic and heterotropic allosteric interactions in metal sensor proteins as well as the steps required to remove the influence of complex speciation from the measured parameter values.

Key words: Metalloregulation, Metal sensor protein, Metals in biology, Isothermal titration calorimetry, ITC, Allosteric coupling free energy

1. Introduction

Allostery is the simple idea that binding of an effector molecule can influence the chemistry or reactivity at another, often spatially distinct, site (1, 2). This communication has evolved as a necessary feature of a wide variety of biological macromolecules and is essential for proper cellular function. Cellular sensory machinery, e.g., transcriptional regulatory proteins, takes advantage of this phenomenon by enabling communication between an effector binding site and a DNA binding interface such that occupancy of the effector site influences the affinity of the protein for its DNA operator. While other chapters in this book focus on other facets

Aron W. Fenton (ed.), *Allostery: Methods and Protocols*, Methods in Molecular Biology, vol. 796,
DOI 10.1007/978-1-61779-334-9_3,

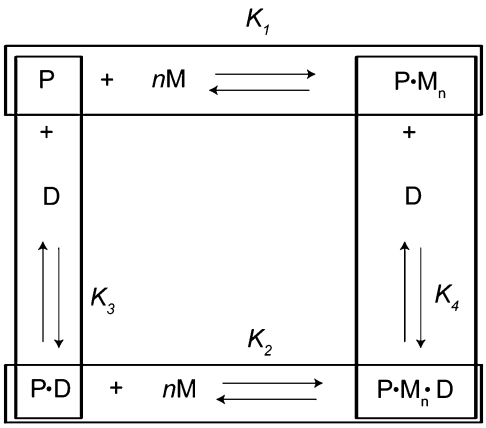

Fig. 1. Heterotropic allosteric coupling scheme. This general four-state thermodynamic cycle accounts for the possible states that a theoretical metalloregulator P can adopt. The vertical and horizontal boxes are the two equilibrium pairs that can be measured to determine the overall allosteric coupling energy, ΔG_C, as described in the text and the four equilibrium constants, along with concentration, dictates the population of each state. The horizontal reactions are defined by n metal (M) ions interacting with the apoprotein (P) or protein–DNA complex (P·D) to form a metallated protein (P·M_n) or the ternary metal–protein–DNA complex (P·M_n·D), respectively, while the vertical equilibria show the possible interactions the DNA (D) can have with P and P·M_n.

of measuring allostery ranging from specific techniques to mapping the communication pathway, this chapter develops a general approach to quantify the thermodynamic forces that govern communication between one binding site and another. We specifically focus on metalloregulatory or "metal sensor" proteins, a specialized class of allosteric transcriptional regulators, which are characterized by many features that make these proteins ideal models for understanding allosteric communication (3). These proteins, like other families of transcriptional regulators, provide an opportunity to observe two types of allosteric communication: heterotropic, which is the communication between the metal regulatory site and the DNA binding interface, and homotropic, which derives from the observation that identical metal-binding sites on homooligomeric proteins are characterized by distinct thermodynamic properties.

1.1. Heterotropic Allosteric Coupling

The widely accepted and applied model of allostery (4) that is drawn upon for this review is depicted in Fig. 1. This model is characterized by closed thermodynamic cycle ($\sum_{i=1}^{4} \Delta X_i = 0$, where X is any thermodynamic state function) with the four corners representative of the four states that a homooligomeric protein (P) can theoretically adopt. When the allosteric protein is a metalloregulator, these are the apoprotein, P, the fully metal coordinated protein with n metal-binding sites filled, P·M_n, an operator DNA associated state for the apoprotein, P·D, and the ternary complex, P·M_n·D, where the protein is fully

coordinated by both metal and DNA ligands. The magnitude of the equilibrium constants, K_i, that describes the transition between these four states dictates the biological role of a metalloregulator. For example, if $K_4 >> K_3$, the P·M_n·D and P states are stable in solution and the protein represses metal uptake upon binding to the cognate metal ion, M. Alternatively, in the cases that $K_3 >> K_4$, the P·M_n and P·D states are biologically relevant and the regulator is likely involved in derepression of the transcription of genes that encode proteins involved in efflux or detoxification of the cognate metal ion, M (3, 5, 6).

This scheme provides a general means to determine the degree to which an effector molecule influences the affinity of a metal sensor protein for the DNA operator, i.e., the degree to which the regulatory protein allosterically couples the two distinct ligand binding sites. When considering the discussion above, it can be concluded that this coupling free energy, ΔG_C, is related to the relative magnitudes of these two equilibrium constants. Indeed, the coupling energy is extracted from the ratio

$$K_C = \frac{K_4}{K_3} = \frac{K_2}{K_1} = \frac{[P][P \cdot M_n \cdot D]}{[P \cdot D][P \cdot M_n]} \quad (1)$$

and describes the ligand exchange equilibrium

$$P{\cdot}M_n + P{\cdot}D \rightleftharpoons P + P{\cdot}M_n{\cdot}D \quad (2)$$

This is perfectly consistent with the example given above. When $K_4 >> K_3$, the products of Eq. 2 are favored. As Eq. 1 shows, this comparison can also be made between the overall metal-binding equilibria, K_1 and K_2, which suggests that quantifying the allosteric coupling between metal binding and DNA binding can be accomplished if either pair of equilibria (vertical or horizontal boxes in Fig. 1) can be measured. It then follows that the coupling free energy, $\Delta G_{C,}$ is simply calculated from the thermodynamic relationship in Eq. 3 and can be further described according to other fundamental thermodynamic relationships (Eqs. 4–5).

$$\Delta G_C = -RT \ln K_C, \quad (3)$$

$$\Delta H_C = \Delta H_4 - \Delta H_3 = \Delta H_2 - \Delta H_1, \quad (4)$$

$$\Delta S_C = \Delta S_4 - \Delta S_3 = \Delta S_2 - \Delta S_1, \quad (5)$$

In the simplified scheme developed above, K_1 and K_2 describe the overall reaction and are, therefore, products of the stepwise equilibrium constants, K_aK_b,...K_n defined by units of M^{-n}. Thus, to explicitly consider stepwise binding constants, K_a, K_b,....K_n, the simplified cycle in Fig. 1 needs to be expanded to include these additional equilibria, as shown in Fig. 2. Note that this scheme with $n = 2$ contains two overlapping $n = 1$ allosteric cycles,

corresponding to the first and second metal-binding events, which are highlighted by the gray and white boxes, respectively. It then follows that *if* the two sequential metal-binding events are considered a single overall event (β_{M2} and β_{MD2}, where $\beta_{M2} = K_{M1} \cdot K_{M2}$ and β_{M2} and β_{MD2}, where $\beta_{MD2} = K_{MD1} \cdot K_{MD2}$), the coupling cycle collapses to that described in Fig. 1 (see Note 1). Calculating the allosteric energies for the individual cycles (gray and white boxes in Fig. 2) can be accomplished exactly as described for the simplified $n = 1$ case, with the inclusion of the additional equilibria in the overall cycle in Fig. 2

$$K_C = \frac{K_{DNA3}}{K_{DNA1}} = \frac{\beta_{MD2}}{\beta_{M2}} = \frac{[P][P \cdot M_2 \cdot D]}{[P \cdot D][P \cdot M_2]}, \tag{6}$$

where K_C describes the ligand exchange reaction

$$P \cdot M_2 + P \cdot D \rightleftharpoons P + P \cdot M_2 \cdot D \tag{7}$$

and the coupling enthalpy and entropy are calculated with

$$\begin{aligned} \Delta H_C &= \Delta H_{DNA3} - \Delta H_{DNA1} \\ &= (\Delta H_{MD1} + \Delta H_{MD2}) - (\Delta H_{M1} + \Delta H_{M2}), \end{aligned} \tag{8}$$

$$\begin{aligned} \Delta S_C &= \Delta S_{DNA3} - \Delta S_{DNA1} \\ &= (\Delta S_{MD1} + \Delta S_{MD2}) - (\Delta S_{M1} + \Delta S_{M2}). \end{aligned} \tag{9}$$

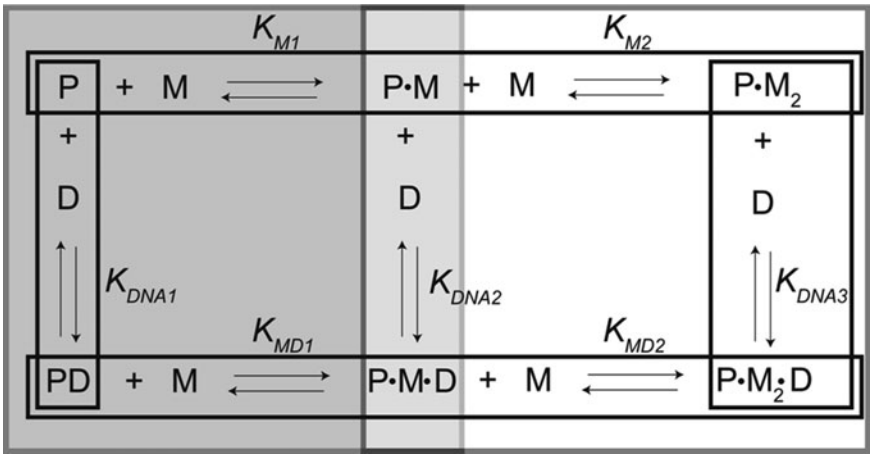

Fig. 2. Expanded heterotropic allosteric coupling scheme. This general six-state thermodynamic cycle accounts for the four allosteric "end" states a homodimeric metalloregulatory protein (P) can hypothetically adopt: apo (P), metal-bound ($P \cdot M_2$), DNA-bound apoprotein ($P \cdot D$) and a "ternary" protein–metal–DNA complex ($P \cdot M_2 \cdot D$). In addition, two intermediate states are shown corresponding to the singly metallated protein ($P \cdot M$) and "ternary" complex ($P \cdot M \cdot D$). The *outer vertical and horizontal boxes* are the two equilibrium pairs that can be measured to determine the overall allosteric coupling energy, ΔG_C, as described in the text. The *gray and white boxes* highlight the thermodynamic cycles that can be used to determine the stepwise coupling energies for the individual metal ions.

1.2. Homotropic Allosteric Coupling

Homotropic allostery in transcriptional regulators is specific to proteins, commonly homodimeric, that contain at least two identical effector binding sites, as represented in the two horizontal equilibria in Fig. 2. If the binding of the first ligand influences the thermodynamic properties of the second binding event, then this system exemplifies homotropic allostery. Measuring this form of allostery is particularly convenient since it can be observed in a single metal-binding experiment, as can be seen in the representative titration in Fig. 3. This titration clearly shows two metal ions,

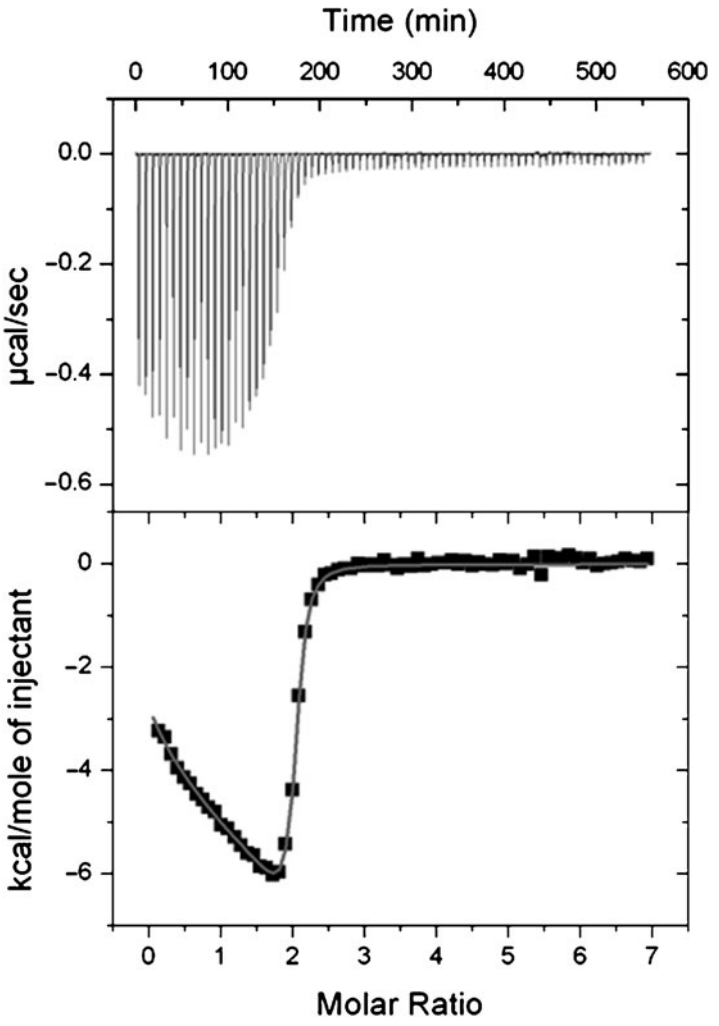

Fig. 3. Representative ITC titration indicative of negative allosteric communication between two identical binding sites on a homodimer. 1.4 mM Zn^{2+} titrated into 34 μM CzrA dimer in 50 mM ACES and 400 mM NaCl at 25°C and pH 7.0 (15). The *top panel* show the raw ITC data with each peak corresponding to an individual 3 μL injection (first injection is 1 μL) plotted as power vs. time. The *bottom panel* show the integrated, concentration normalized data plotted as ΔH vs. the Zn^{2+}-CzrA dimer molar ratio. Here, we see that each CzrA dimer binds two nonequivalent Zn^{2+} ions with negative cooperativity; however, this system is interestingly characterized by a homotropic coupling enthalpy, ΔH_C, that opposes ΔG_C. This feature has been observed in other allosteric regulators (31).

M_1 (Zn_1) and M_2 (Zn_2), binding to a protein (CzrA) with distinct nonequivalent thermodynamics, exemplifying homotropic allosteric communication. Since standard fitting procedures do not account for this necessary statistical feature, it is essential to correct the macroscopic binding constants, K_{M1} and K_{M2} (or K_{MD1} and K_{MD2}). This is accomplished by casting the K_{M1} and K_{M2} in terms of a single microscopic binding event, k, and a cooperativity term, ω, with a factor of 2 included to account for the two statistically equivalent metal-binding sites, as demonstrated in Eqs. 10–12 (7).

$$K_{M1} = 2k, \tag{10}$$

$$K_{M2} = \frac{\omega k}{2}, \tag{11}$$

$$\Delta G_C = -RT \ln \omega = -RT \ln \frac{4K_{M2}}{K_{M1}}. \tag{12}$$

According to this analysis, ω is the microscopic coupling constant and its magnitude dictates the degree to which two homotropic binding events are coupled. When $\omega > 1$, the binding of the first ligand increases the affinity of the 2nd ligand (positively cooperative) and, conversely, when $\omega < 1$, the system is characterized by negative cooperativity. The enthalpic and entropic coupling energies for homotropic interactions can be calculated from Eqs. 13 and 14, respectively.

$$\Delta H_C = \Delta H_{M2} - \Delta H_{M1}, \tag{13}$$

$$\Delta S_C = \frac{-\Delta G_C + \Delta H_C}{T}. \tag{14}$$

2. Materials

1. The ultimate goal of the approach outlined here is to quantify the global thermodynamics that drive allosteric processes. Therefore, a sensitive microcalorimeter is necessary. Two common commercial sources for this instrument are MicroCal, LLC. (Northampton, MA) and TA Instruments (Lindon, UT), respectively. In addition to the standard 1.4 or 1 mL reaction cell volumes, each of these suppliers also offer a more contemporary model that minimizes sample volume (~200 μL) and increases absolute sensitivity (8) (see Note 2).
2. Reagents of the highest purity are strongly recommended since even modest contamination can significantly influence the solution properties of metal ions. High-purity standard biological reagents (buffers, etc.) are typically available

from a variety of suppliers (e.g., Sigma, Fisher, VWR). Most metal salts are available in ultra high purity grade from Alfa Aesar.

3. If anaerobic conditions are necessary, appropriate oxygen free chambers are necessary for sample preparation and calorimetric measurement.
4. DNA binding and metal into protein/DNA complex titrations requires duplex DNA corresponding to the native operator sequence. Single stranded DNA oligonucleotides are commercially available in high purity from a number of commercial sources including Operon (Huntsville, AL) and IDT (Coralville, IA). Following purification (see Note 3), accurately determine ssDNA concentration using the appropriate extinction coefficient (http://www.idtdna.com/analyzer/Applications/OligoAnalyzer/). Anneal the two strands by mixing equimolar concentrations in an eppendorf tube and heating to 95°C followed by slowly cooling to room temperature, with DNA duplex formation confirmed by native polyacrylamide gel electrophoresis. Care must be taken to avoid fold-back intramolecular DNA hairpin structures that might arise from the palindromic or nearly palindromic and, therefore, self-complementary nature of the individual ssDNA strands (see Note 4). DNA duplexes prepared in this way at high strand concentrations are stored at −20°C and are stable indefinitely.
5. Protein preparation should be carried out by standard protocols (see Note 5). It is recommended that samples estimated to be ≥ 95% pure by SDS-PAGE are used.

3. Methods

3.1. Solution Condition Considerations

Conditional variability can appreciably influence the heat measured by bulk thermodynamic techniques such as ITC. It is, therefore, of paramount importance to select appropriate solution conditions. Listed below are a number of conditional variables that should be specifically addressed. Note that this is not an exhaustive list and additional considerations should be identified on an individual experimental basis. In general, it is recommended to select solution conditions that generate quantifiable speciation to enable robust mathematical analysis.

1. *pH*. In addition to the obvious effects of pH on biological macromolecules (e.g., acid/base catalyzed hydrolysis), pH can significantly influence the solution properties of cationic metals. For example, at basic or neutral pH, $Fe(OH)_3$ is

sparsely soluble ($K_{sp} = 2.64 \times 10^{-39}$ M^2 (9)). The ideal pH would mimic the conditions that dictate the chemistry in vivo. Note that the pH can significantly influence the apparent affinity, as discussed later.

2. *Buffer.* The obvious criterion for buffer selection is to maintain a constant pH. However, when transition metal ions are of interest, metal-buffer equilibria must be considered explicitly since nearly all buffers associate with metal ions to some degree (10, 11), although a number of these are very weakly coordinating (12). It is also notable that some buffers promote redox activity through stabilization of one oxidation state relative to another, e.g., copper (13). As noted above, it is recommended to use buffers that are characterized by quantifiable metal-buffer affinity and speciation so as to limit unquantifiable metal solution chemistry. A number of resources are available to guide the reader to buffers with metal chemistries rigorously quantified (10, 11). If the experiment necessitates a specific buffer and thermodynamic information is not available for this system, these values may be determined calorimetrically using the guidelines provided below (14–17). Some experiments require the presence of a strong metal chelator to enable measurement of a quantifiable binding curve (vida infra); in these cases the metal-buffer interaction may become insignificant.
3. *Ionic Strength.* The ionic strength (I) of a solution directly influences the activity coefficient, and hence the measurable equilibrium constant. Eq. 15 shows Debye–Hückel relationship which indicates that I is a function of the total ionic content and scales with the square of the valency (z_i) for each species (i).

$$I = 1/2 \sum_i z_i^2 [i] \tag{15}$$

In theory, all ions in solution should be included in this calculation; however, under typical experimental conditions (50–500 mM monovalent salt concentration (see Note 6)), the contribution from metal salts and ligand are commonly negligible, although it may be necessary to consider the influence of the buffer at elevated concentrations. High concentrations of DNA, as well as its counter ion, can have a very significant impact on ionic strength; however, the simple relationship presented in Eq. 15 cannot describe polyelectrolyte contributions appropriately; a nonlinear Poisson–Boltzmann analysis is necessary for accurately accountability (18). Owing to the difficulty of these calculations, and typically minor influence it has on the data, they are commonly

ignored. 100 mM monovalent salt has commonly been used for metal-binding experiments (11) and provides a standard for direct comparisons between different systems.

4. *Temperature.* Equilibrium constants are inherently temperature-dependent and most biological processes are characterized by $\Delta C_p \neq 0$ resulting in ΔH variance with temperature. Since K_i and ΔH are the two directly measurable variables in an ITC experiment, temperature is a very important experimental variable. Fortunately, modern calorimeters maintain a constant temperature (~4–80°C) over the course of very long experiments. Therefore, one only needs to decide the most appropriate temperature for the system of interest, with 25 and 37°C commonly employed.
5. *Oxygen Sensitivity.* Owing to the largely reducing potential of most intracellular environments, metal ions and surface cysteines tend to be in a reduced state, i.e., Cu^+ and Cys-SH or Cys-S^- as compared to Cu^{2+} and Cys-S–S-Cys. For systems that are susceptible to metal and/or ligand oxidation, anaerobic preparation and experimentation is strongly advised. The use of "pseudo-anaerobic" or chemically reducing conditions is fraught with serious shortcomings. Most common reducing agents interact with metal ions with significant affinities, with dithiothreitol (DTT) being the dramatic particularly notable case as many metal ions make very high-affinity metal–DTT complexes (11, 19). These complexes outcompete the desired metal–protein interactions, particularly in light of the large molar excess relative to protein that is necessary for these experiments. Further, comprehensive control experiments are required to verify that the unavoidable redox chemistry in an aerobic environment, e.g., reducing agent oxidation, does not influence the net heat flow (i.e., the measurable variable). For these reasons, it is strongly advised that oxygen-sensitive experiments be conducted under strictly anaerobic conditions in the absence of chemical reductants (see Subheading 3).

3.2. Metal-Free Buffers

As this guide is geared toward quantifying metal-ion-driven chemistries, it is necessary to ensure that all materials are prepared in a way to minimize contamination. For systems not focusing on metals, the guidelines below are still worthwhile, as they ensure minimal interference from extraneous sources.

1. *Preparation of Glassware.* Standard silicate laboratory glassware is very susceptible to metal contamination. This is particularly true for "hard" metals (i.e., Fe^{3+} and Mg^{2+}), which form strong electrostatic interactions with anions

(20). Metalloregulatory proteins, which can possess very high affinities for their cognate metal ion (3, 21), can, therefore, leach metals from contaminated glass surfaces. This is easily avoided by ensuring that all glassware is soaked in 1% nitric acid (HNO_3) enabling protons to outcompete metal ions at the surface. Following acid treatment, the glassware should be rinsed exhaustively ($\geq 3\times$) with metal-free water (see below) to avoid an unwanted change in the pH of buffer solutions.

2. *Metal-Free Water*. Standard RODI water purification, common in most research laboratories, is not sufficient to remove metal ions to the degree required for quantitative metal-binding experiments. Further purification can be provided by numerous standard purification systems that are capable of deionization to a resistance ≥ 18 MΩ cm. Alternatively, strong metal chelators conjugated to solid styrene beads are commercially available, i.e., Chelex, and can be used to treat laboratory-grade RODI water to produce operationally defined "metal-free" water. This can be accomplished by passing water through a vertical column containing chelating resin and collecting it in an acid-washed container. Alternatively, the resin can be added directly into the water and shaken for several hours. Incubation at elevated temperatures can expedite this procedure. Separate the phases by centrifugation and careful decanting.
3. *Buffer Preparation*. Buffer salts, as provided by the manufacturer, are commonly contaminated with small amounts of divalent metal ions. Removal of metal ions can easily be accomplished by treating the prepared buffer with Chelex, as described just above. Note that Na^+ or H^+ ions (depending on the regeneration protocol used for the Chelex resin) replace the metals to maintain electrostatic neutrality and, depending on the amount of metal removed from the buffer, this may be significant. pH and conductivity measurements of the post-Chelex solution are strongly suggested.

3.3. Anaerobic Preparations

For cases that require extra care to minimize oxidative conditions as discussed in Subheading 1, additional steps must be taken to ensure a rigorously anaerobic environment, since thoroughly deoxygenated buffers and solutions are required by these experiments.

1. Prepare the buffer solution using metal-free water and remove residual metal as necessary (see Subheading 2).
2. Two standard degassing protocols are available to ensure that all solutions are free of oxygen. The first method is more

rapid, but has the potential for mild increase in salt and buffer concentration due to water evaporation (see Note 7), while the second is much more thorough and minimizes solvent evaporation (see Note 8).

3. Stock metal solutions should be prepared and stored under an inert atmosphere. The simplest method is to dissolve a known mass of metal salt in an anaerobic chamber (Vacuum Atmospheres or Coy). If an anaerobic chamber is not available, deoxygenation can be accomplished suboptimally by extensive bubbling of argon or nitrogen from a cylinder of compressed gas through a metal stock solution. The concentration of this stock solution should be verified by standard metal quantification techniques prior to use.
4. Completely buffer exchange the purified protein into an oxygen-free buffer. This is accomplished by concentrating the protein stock to ~12 mL, transferring to an anaerobic chamber and dialyzing at least 4 h in 500 mL of the buffer to be used to metal-binding experiments. The dialysis buffer should be exchanged four times to ensure complete removal of oxygen and metal chelators or reducing agents that may have been used during protein purification.

3.4. Metal-Binding Assays

In general, many experimental design considerations are discussed in detail in instrument manuals (22) and any user should be familiar with these publications. It is recommended that titrations are designed that involve well-defined metal–chelator interactions, as direct titrations involving "free" metal ions pose a number of potential problems. Some common examples of useful chelators include nitrilotriacetic acid (NTA), imidazole, triethylenetetramine (trien), ethylenediamine (en), and Tris buffer; however, note that different degrees of competition are elicited by each of these(10, 23) (vida infra). As mentioned above, unknown solution chemistry may be occurring that cannot be appropriately accounted for. Further, it is highly unlikely that metal ions are present in a cellular environment not associated with a cellular chelator. Second, it is quite likely that a direct titration of metal → protein lies outside of the experimental window that allows for a robust fit to a unique binding constant. An example titration of Zn^{2+} into CzrA, a homodimeric Zn^{2+}/Co^{2+} sensor from *Staphylococcus aureus*, is shown in Fig. 3.

1. Ensure that the calorimeter is well maintained, calibrated, and operating properly. Refer to the instrument manual for specific directions.
2. Prepare at least 2 mL of 10–100 μM protein in a predetermined experimental buffer. Ensure that the buffer is metal free as described in Subheading 2. At least four rounds

of dialysis are recommended. The dialysis buffer from the last round should be saved to prepare the metal solution and used in the reference cell of the calorimeter.

3. Prepare at least 1 mL of 1 mM (see Note 9) metal salt from a stock solution (see Note 10) in the appropriate experimental buffer. It has been our experience that preparing extra (~10 mL) metal titrant solution is ideal because it enables concentration determination (via AAS or ICP-MS) of this solution eliminating error arising from dilution. To ensure that the buffer exactly matches the protein buffer, the buffer from the final protein dialysis step may be used.
4. Ensure that the calorimeter has been thoroughly cleaned (see Note 11).
5. Rinse the sample cell and titration syringe with the experimental buffer.
6. Load the titration syringe, sample cell, and reference per manufacturer's recommendations.
7. Insert the appropriate experimental parameters. An iterative process is likely required to determine the ideal parameter values. While the experiment is running, pay close attention to the injection volumes, as large injections may mask data inflections, and make fitting impossible or inaccurate (see Note 12). If the instrument cycle is complete before the reaction has reached completion, it may be possible to refill the syringe and continue the experiment (this can be done multiple times if necessary, refer to instrument specifications). Once all data are acquired, the files can be concatenated. MicroCal has developed software to automate this procedure.
8. Repeat the experiment at least two more times. Make appropriate adjustments to the experimental parameters.

If the goal is to quantify the heterotropic coupling energy, this set of experiments must be repeated with the protein–DNA complex. Duplex DNA preparation is described in Subheading 2. Note that this measurement may be very challenging unless very high concentrations can be reached in cases where the affinity of the ternary $P{\cdot}M_n{\cdot}D$ complex is low. It is strongly urged that the investigator show that all of the protein be quantitatively contained in the protein–DNA complex after the completion of the metal-binding experiment (15).

1. Select a gel filtration column capable of separating dsDNA and the metal-bound or apo protein complex from the protein–DNA complex. Pass each of these solutions across the column to generate a retention volume profile for the system of interest.

2. Collect the contents of the reaction cell once the reaction has reached completion. Take all necessary precautions regarding specific techniques necessary for the system (i.e., anaerobic).
3. Load the sample on the calibrated gel filtration column, making sure to monitor the absorbance at 260 nm and 280 nm. If the protein of interest has a low molar extinction coefficient, monitor at 240 nm as well.
4. Collect the appropriate fractions.
5. Quantify the total metal concentration contained in these two samples.
6. Calculate the total metal–protein stoichiometry for the two samples, ensuring an accounting for dilution.

3.5. Accounting for Speciation

3.5.1. Adjusting the Binding Constant

Metal speciation, which comprises metal interactions with other solutes to form multiple metal–solute complexes, is unavoidable under the solution conditions necessary to conduct these experiments. Standard ITC data fitting packages cannot account for these competing equilibria. It is, therefore, necessary to correct the optimized thermodynamic parameters obtained by fitting the experimental data to a standard physical model(s). Provided the experiment is carefully designed, all competing interactions with these solutes, which can be any experimental buffer salt (e.g., Tris) or low-affinity metal chelator (e.g., NTA), collectively referred to as "B" here (see Note 2), are known and readily accounted for as described below. For the purpose of this exercise, it is assumed that the metal interacts with the experimental buffer (B) to form two metal-buffer species, MB and MB_2, where B is the form of the buffer that complexes with the metal ion, likely the fully deprotonated form, and the higher affinity ligand, L, is present as a single molecular species. This approach can easily be extended to more complex systems that explicitly consider ligand (L) protonation chemistry that is likely to occur over the biological pH range (see Note 13) as described below (Eq. 24 is a representative equilibrium).

Consider the following expression:

$$(1-\alpha_{MB}-\alpha_{MB2})M+\alpha_{MB}MB+\alpha_{MB2}MB_2+L\rightleftarrows ML + (\alpha_{MB}+2\alpha_{MB2})B \quad (16)$$

In this expression, α_{MB} and α_{MB2} are the stoichiometric coefficients associated with MB and MB_2, respectively, and determined from the individual equilibrium constants, K_i or β_i (see Notes 1 and 14).

$$\alpha_{MB}=\frac{[MB]}{C_M}=\frac{K_{MB}[B]}{\alpha_{Buffer}}, \quad (17)$$

$$\alpha_{MB2} = \frac{[MB]}{C_M} = \frac{\beta_{MB2}[B]^2}{\alpha_{Buffer}}, \tag{18}$$

$$\alpha_{Buffer} = 1 + K_{MB}[B] + \beta_{MB2}[B]^2. \tag{19}$$

The standard *one-site* fitting model assumes a direct interaction between metal (M) and ligand (L) according to

$$M + L \rightleftharpoons ML, \tag{20}$$

$$K_{cal} = \frac{[ML]}{[M][L]}. \tag{21}$$

This assumption ensures that all metal ions are present as the free hydrated metal (M) or associated with the macromolecular ligand L such that

$$K_{cal} = \frac{[ML]}{(C_M - [ML])(C_L - [ML])} = \frac{[ML]}{[M][L]}, \tag{22}$$

where C_M and C_L are the total metal and ligand concentrations, respectively. This, of course, is not the case for the chemical system described by Eq. 16. Therefore, Eq. 22 must be expanded to account for the additional chemical species that are present in the reaction.

$$\begin{aligned} K_{cal} &= \frac{[ML]}{(C_M - [ML])(C_L - [ML])} \\ &= \frac{[ML]}{\left(1 + K_{MB}[B] + \beta_{MB2}[B]^2\right)[M][L]} = \frac{K_{ML}}{\alpha_{Buffer}}. \end{aligned} \tag{23}$$

It then follows that the apparent binding constant, K_{cal}, can be converted to the competition-independent value, K_{ML}, by simply multiplying it by the metal-buffer reaction quotient, $\alpha_{Buffer.}$ If it is necessary to account for acid–base equilibria of the ligand, L, a corresponding competition value may be added to this expression (see Note 13).

3.5.2. Adjusting the Enthalpy

To extract the enthalpy change associated with metal–ligand interactions of interest, and the corresponding protein structural or dynamic response (Eq. 20), collectively ΔH_{ML}, the heats associated with the coupled chemical events must be subtracted from the measured calorimetric enthalpy, ΔH_{cal}. To accomplish this, Hess' Law is applied to the overall equilibrium which enables the isolation of individual equilibria that contribute to the net evolved heat. For this example, we extend the equilibrium in Eq. 16 to include a single protonation/deprotonation event on the ligand since subtraction of proton-buffer heats is required.

$$(1-\alpha_{MB}-\alpha_{MB2})M+\alpha_{MB}MB+\alpha_{MB2}MB_2+(1-\alpha_{HL})L+\alpha_{HL}HL \rightleftarrows ML+(\alpha_{MB}+2\alpha_{MB2}-\alpha_{HL})B+\alpha_{HL}HB, \quad (24)$$

$$\alpha_{HL}=\frac{[HL]}{C_L}=\frac{K_{HL}[H]}{\alpha_{Proton}}, \quad (25)$$

$$\alpha_{Proton}=1+K_{HL}[H]. \quad (26)$$

To begin the disassembly of Eq. 24, we consider three categories of equilibria: those involving metal–buffer (MB_i) interactions (Eqs. 27–28), those involving proton flow (Eqs. 29–30), and finally the desired metal–ligand interaction (Eq. 31). Note that these equations are written such that they sum up the overall equilibrium and Eqs. 27–29 are the reverse of the association reaction; therefore, a negative sign must be placed in front of standard state functions to describe the equations as written, as indicated.

$$\{MB \rightleftharpoons M+B\}\alpha_{MB}-\alpha_{MB}\Delta H_{MB}, \quad (27)$$

$$\{MB_2 \rightleftharpoons M+2B\}\alpha_{MB2}-\alpha_{MB2}\Delta H_{MB2}, \quad (28)$$

$$\{HL \rightleftharpoons L+H\}\alpha_{HL}-\alpha_{HL}\Delta H_{HL}, \quad (29)$$

$$\{B+H \rightleftharpoons HB\}\alpha_{HL}-\alpha_{HL}\Delta H_{HB}, \quad (30)$$

$$M+L \rightleftharpoons ML-\Delta H_{ML}. \quad (31)$$

According to this scheme, the desired heat associated with Eq. 31 (ΔH_{ML}) can be calculated by subtracting the heat from Eq. 27 through Eq. 30 from the overall measured enthalpy, ΔH_{cal}.

$$\Delta H_{ML}=\Delta H_{cal}+\alpha_{MB}\Delta H_{MB}+\alpha_{MB2}\Delta H_{MB2}+\alpha_{HL}\Delta H_{HL}-\alpha_{HL}H_{HB}. \quad (32)$$

However, this necessitates a priori knowledge of all these values. While this is readily done for ΔH_{HB} from literature sources, the specific set of conditions influences all of the other competing equilibria. Therefore, it is necessary to experimentally determine each of these. As a representative example, the protocol below employs the well-characterized metal–EDTA interactions (11) to determine the total metal-buffer heat, which is the sum of the individual metal–buffer interactions, as shown in Eq. 33.

$$\Delta H_{MBtot}=-(\alpha_{MB}\Delta H_{MB}+\alpha_{MB2}\Delta H_{MB2}). \quad (33)$$

1. Ensure cleanliness and proper operation of the calorimeter (see Note 11).
2. Prepare at least 2 mL of 100 μM (see Note 10) EDTA in an identical buffer used for the metal–protein titration.
3. Prepare at least 1 mL of 1 mM (see Note 9) metal salt in identical experimental buffer.
4. Conduct the titration using the appropriate instrument settings. It is recommended to use the same settings as that for the metal–protein titration. Ideally, a step function is observed; consider a tighter binding ligand if this is not the case.
5. Repeat at least twice.
6. Average the measured heats. Propagate error appropriately (24).
7. Calculate α_{HL} and α_{H2L}, and α_{Proton} (see Note 15) from $K_{HL} = 10^{9.52}$ and $\beta_{H2L} = 10^{15.65}$ for EDTA (the ligand (L) in this case).
8. Calculate ΔH_{MBtot} according to

$$\Delta H_{MBtot} = \Delta H_{cal} - \alpha_{HL}(\Delta H_{HB} - \Delta H_{HL}) - -\Delta H_{ML}. \quad (34)$$

This can then be used to subtract ΔH_{MBtot} from any reaction under identical conditions (i.e., Eq. 32). Further, this set of equations and approach is completely generic and can be applied to any metal–ligand interaction assuming that adjustments are made in each category for additional (or fewer) species.

3.5.3. Determining Protons Displaced Calorimetrically

As described above, due to the dramatic influence buffer–proton interactions can have on the overall ΔH, it is necessary to subtract this value from ΔH_{cal}. To accomplish this correctly, the net number of protons displaced or taken up (n_{H+}) must be known.

$$n_{H+} = \sum_i i\alpha_{HiL}. \quad (35)$$

If all relevant pK_as are known, this value can easily be calculated according to Eq. 29 and the experimental pH; however, for biological macromolecules, it is likely that it needs to be experimentally determined. While this can be accomplished by other methods (25), determining this value calorimetrically provides additional thermodynamic data and makes the optimized parameter values more statistically robust. This method (26, 27) is based on the fact that under identical conditions of pH, salt concentration and type, and temperature, changing the buffer (B) leads only to a change in the heat associated with the buffer chemistry; for the case at hand, this includes metal–buffer and proton–buffer interactions.

1. Select three or more buffers that maintain a constant pH at the experimental pH of interest, with each characterized by a significantly different ΔH_{HB} (11).
2. Prepare the protein and buffer taking the necessary precautions to ensure otherwise identical solution conditions and using the same batch of protein stock as before if possible.
3. Determine ΔH_{MBtot}, as described in Subheading 5.2. Note that some metal–buffer pairs can influence the ligand exchange kinetics; therefore, keenly monitor the first few injections as well as the injections nearing stoichiometric equivalence to be sure that equilibrium is attained after each injection (see Note 12).
4. Conduct metal → protein titrations in triplicate in the each buffer, again taking care to ensure that all experiments are carried out at the same temperature while monitoring the progress of successive injections (see Note 12).
5. Repeat this procedure with more buffers as needed. At least three buffers are required for a robust determination of the n_{H+}.

Once the data are collected and the metal–buffer interactions are subtracted, a plot of ΔH_{HB} vs. $\Delta H_{cal} - \Delta H_{MBtot}$ generates a straight line with the slope corresponding to the number of protons displaced (or consumed), n_{H+}, under this specific set of solution conditions, according to

$$(\Delta H_{cal} - \Delta H_{MBtot}) = n_{H+}\Delta H_{HB} + (\Delta H_{ML} + \Delta H_{HLtot}), \quad (36)$$

where ΔH_{HLtot} is the total enthalpy associated with proton–ligand interactions and ΔH_{ML} + ΔH_{HLtot} is the heat associated with the metal–protein interaction and coupled proton release, both of which are constant throughout this series of experiments.

4. Notes

1. Standard equilibrium nomenclature defines β as an overall binding constant and is, therefore, the product of sequential equilibrium constants (e.g., $\beta_{MB2} = K_{MB}K_{MB2}$). Ensure that the equilibrium constants used for these calculations describe the association equilibria. For example, in the generic reaction

$$X + Y \rightleftharpoons XY$$

$$K = [XY]/[X][Y]$$

2. Standard nomenclature for ITC experiments, as used in MicroCal, LLC VP-ITC user manual (23), refers to the molecule in the injection syringe as the *ligand* (L) and the molecule in the reaction cell as the *macromolecule* (M). However, to remain consistent with common metal speciation nomenclature (11), in this manuscript we explicitly use M to refer to the *metal ion* and L refers to the *ligand* that binds to the metal ion in which the heat of association is measured. In our examples, we use L to indicate either protein or EDTA and include B as a representative molecule that interacts with the metal ion at a lower affinity than the *ligand* of interest in a competitive manner.
3. Large quantities of DNA are needed for these experiments, particularly given the standard 1.0 or 1.4 mL reaction volumes of the nanoITC (TA) or VP-ITC (MicroCal) , respectively. Several 1 μmol scale DNA syntheses are likely needed to generate adequate material for these experiments. Single-stranded DNAs are routinely purified by denaturing PAGE followed by electroelution ($l > 20$ nts) or high resolution anion exchange chromatography ($l \leq 20$ nts), and ethanol precipitation. In the case of denaturing PAGE-purified DNAs, complete removal of acrylamide and urea is ensured by a final reverse phase clean up step using prepacked C18 columns (Alltech) and elution with 50% methanol. Dry to completeness with a SpeedVac.
4. Some duplex DNA operator sequences are palindromic or twofold symmetric or nearly so. As a result, a ssDNA hairpin may be thermodynamically favored over the intermolecular dsDNA. Strand annealing under conditions of high monovalent salt concentration (0.5–1 M NaCl) promotes duplex formation. Additionally, increased strand concentration may be needed to favor the intermolecular duplex formation. Note that rapid cooling should be avoided, as this process favors hairpin formation.
5. Since metal-binding events are of particular interest, it is strongly advised that purification by His-tags is avoided. Obviously, high-affinity interactions between these motifs and metal ions can obscure the metal-binding events of functional interest.
6. Elevated monovalent salt concentration in these systems is often required to enhance protein solubility. Further, if the protein–DNA interactions are of interest, high salt is often needed to ensure that the affinities are within the measurable range due to the sizeable electrostatic contribution to K_a for essentially all protein–DNA interactions (28–30). For a direct

comparison of binding affinities between different systems, the solution conditions must be identical.

7. Transfer/prepare the buffer in a 2–3 L round bottomed vacuum flask (a reaction flask from Kontes works well for this purpose). Attach the flask to a dual line manifold with one dedicated vacuum line and the other attached to a cylinder of argon. Situate the flask on a magnetic stirring mechanism and stir under high vacuum for at least 1 h/l of buffer (2 /l is recommended). Back-fill with argon. Stir for 1 h/l ensuring that the vessel is sealed. Repeat. Transfer the sealed vessel to an anaerobic chamber. Note that this method leads to a small increase in buffer concentration as a result of unavoidable solvent evaporation.
8. Prepare the buffer in a vacuum flask (typically available up to 500 mL) leaving at least 1/3 of the flask volume empty. Submerge the flask into liquid nitrogen or an isopropanol–dry ice slurry until completely frozen. While still frozen, expose to a high vacuum for 10–20 min. Close the flask and warm until completely melted. Submersion in tepid water can help this process; however, caution is urged to avoid fracturing the glassware as a result of a rapid temperature change. Repeat this process three times followed by backfilling the flask with Argon for transfer to an anaerobic chamber.
9. The concentration can be adjusted if necessary to account for very large or small measured heats or other experimental considerations.
10. Some metals are sparingly soluble at high concentrations unless the solution is acidic (e.g., Fe^{3+}). At a given pH, the soluble metal concentration can be easily calculated from solubility products (9). We tend to prepare $\geq$100 mM stock metal concentrations under neutral conditions if possible for use as titrants. Higher stock concentrations minimize the buffer dilution that occurs upon sample preparation; however, as long as >100 mM concentrations are used, this dilution is insignificant. Regularly verify the stock concentration of metal titrants by atomic absorption spectroscopy or ICP-MS.
11. Although several methods are available for cleaning and ITC, we recommend a protocol consisting of soaking the sample cell and titration syringe in 10 mM EDTA, 1 mM DTT prepared in 0.1% detergent (such as Micro-90) at 65°C for 4 h followed by a thorough rinse with metal-free water (1–2 L)
12. Although monitoring all injection aliquots is a good idea, it is particularly appropriate to monitor the first several injections to verify that enough time is allowed for the signal to return to baseline. Further, the injections leading up to the stoichiometric

equivalence or inflection point should also be monitored due to the reduced concentration of ligand and resulting slower reaction. If enough time is not allowed to verify reaction equilibrium, the data are unreliable.

13. If one desires to account for ligand protonation speciation, a competition term is easily derived: $\alpha_{\text{Proton}} = \sum_{i=0}^{n} \beta_i [H]^i$. However, it should be noted that unless the exact pK_a values are known or can be determined for all titratable groups on the ligand, accounting for acid–base chemistry is largely an approximation. Further, while the heat associated with amino-acid protonation chemistry has been quantified, these values are specific for the free amino acids and, therefore, neglect any local microenvironment, i.e., charge stabilization or dielectric constant. For this reason, these equilibria can be ignored and the results then become pH-specific (15). However, the heat associated with buffer protonation is readily determined and should be accounted for (see Subheadings 5.2 and 5.3)
14. It is assumed that the buffer is in large excess and the concentration is effectively constant.
15. $$\alpha_{\text{Proton}} = 1 + 10^{9.52}[\text{H}] + 10^{15.65}[\text{H}]^2,$$

$$\alpha_{\text{H2L}} = \frac{10^{15.65}[\text{H}]^2}{\alpha_{\text{Proton}}}.$$

References

1. Monod, J., Wyman, J., and Changeux, J.-P. (1965) On the nature of allosteric transitions: A plausible model, *J Mol Biol* ***12***, 88–118.
2. Monod, J., Changeux, J.-P., and Jacob, F. (1963) Allosteric proteins and cellular control systems, *J Mol Biol* ***6***, 306–329.
3. Ma, Z., Jacobsen, F. E., and Giedroc, D. P. (2009) Coordination chemistry of bacterial metal transport and sensing, *Chem Rev* ***109***, 4644–4681.
4. Reinhart, G. D. (2004) Quantitative analysis and interpretation of allosteric behavior, *Methods Enzymol* ***380***, 187–203.
5. Giedroc, D. P., and Arunkumar, A. I. (2007) Metal sensor proteins: nature's metalloregulated allosteric switches, *Dalton Trans*, 3107–3120.
6. Busenlehner, L.S., Pennella, M.A., and Giedroc, D.P. (2003) The SmtB/ArsR family of metalloregulatory transcriptional repressors: structural insights into prokaryotic metal resistance, *FEMS Microbiol Rev 27*, 131–143.
7. Lee, S., Arunkumar, A. I., Chen, X., and Giedroc, D. P. (2006) Structural insights into homo- and heterotropic allosteric coupling in the zinc sensor *S. aureus* CzrA from covalently fused dimers, *J Am Chem Soc* ***128***, 1937–1947.
8. Peters, W. B., Frasca, V., and Brown, R. K. (2009) Recent developments in isothermal titration calorimetry label free screening, *Combinatorial Chemistry; High Throughput Screening* ***12***, 772–790.
9. *CRC Handbook of Chemistry and Physics*, 75 ed., (1994) CRC Press, London.
10. Magyar, J. S., and Godwin, H. A. (2003) Spectropotentiometric analysis of metal binding to structural zinc-binding sites: accounting quantitatively for pH and metal ion buffering effects, *Anal Biochem* ***320***, 39–54.
11. NIST Standard Reference Database 46, Version 7.0.
12. Yu, Q., Kandegedara, A., Xu, Y., and Rorabacher, D. B. (1997) Avoiding interferences from good's buffers: a contiguous series of noncomplexing tertiary amine buffers

covering the entire range of pH 3–11, *Anal Biochem* ***253***, 50–56.

13. Hegetschweiler, K., and Saltman, P. (1986) Interaction of copper(II) with N-(2-hydroxyethyl)piperazine-N′-ethanesulfonic acid (HEPES), *Inorg Chem* ***25***, 107–109.
14. Grossoehme, N. E., Akilesh, S., Guerinot, M. L., and Wilcox, D. E. (2006) Metal-binding thermodynamics of the histidine-rich sequence from the metal-transport protein IRT1 of *Arabidopsis thaliana*, *Inorg Chem* ***45***, 8500–8508.
15. Grossoehme, N. E., and Giedroc, D. P. (2009) Energetics of allosteric negative coupling in the zinc sensor *S. aureus* CzrA, *J Am Chem Soc* ***131***, 17860–17870.
16. Grossoehme, N. E., Mulrooney, S. B., Hausinger, R. P., and Wilcox, D. E. (2007) Thermodynamics of Ni2+, Cu2+, and Zn2+ binding to the urease metallochaperone UreE, *Biochemistry* ***46***, 10506–10516.
17. Grossoehme, N. E., Spuches, A. M., and Wilcox, D. E. (2010) Application of isothermal titration calorimetry in bioinorganic chemistry, *J Biol Inorg Chem* ***15***, 1183–1191.
18. Sharp, K. A., and Honig, B. (1990) Calculating total electrostatic energies with the nonlinear Poisson-Boltzmann equation, *J Phys Chem* ***94***, 7684–7692.
19. Krezel, A., Lesniak, W., Jezowska-Bojczuk, M., Mlynarz, P., Brasuñ, J., Kozlowski, H., and Bal, W. (2001) Coordination of heavy metals by dithiothreitol, a commonly used thiol group protectant, *J Inorg Biochem* ***84***, 77–88.
20. Cotton, A.W., Geoffrey, M., Carlos, A., Bochman, M. (1999) Advanced Inorganic Chemistry, 6 ed., Wiley, New York.
21. Eicken, C., Pennella, M. A., Chen, X., Koshlap, K. M., VanZile, M. L., Sacchettini, J. C., and Giedroc, D. P. (2003) A metal-ligand-mediated intersubunit allosteric switch in related SmtB/ArsR zinc sensor proteins, *J Mol Biol* ***333***, 683–695.
22. MicroCal. (2002) MicroCalorimeter User's Manual, Northampton, MA.
23. O'Halloran, T. (1993) Transition metals in control of gene expression, *Science* ***261***, 715–725.
24. Taylor, J. R. (1997) in An Introduction to Error Analysis 2nd ed., University Science Books, California.
25. Yang, X., Chen-Barrett, Y., Arosio, P., and Chasteen, N. D. (1998) Reaction paths of iron oxidation and hydrolysis in horse spleen and recombinant human ferritins, *Biochemistry* ***37***, 9743–9750.
26. Doyle, M.L., Louie, G., Dal Monte, P.R., and Sokoloski, T.D. (1995) Tight binding affinities determined from thermodynamic linkage to protons by titration calorimetry, ***259,*** 183–194.
27. Baker, B. M., and Murphy, K. P. (1996) Evaluation of linked protonation effects in protein binding reactions using isothermal titration calorimetry, *Biophys J* ***71***, 2049–2055.
28. Record, M.T., Jr., Ha, J.H., and Fisher, M.A. (1991) Analysis of equilibrium and kinetic measurements to determine thermodynamic origins of stability and specificity and mechanism of formation of site-specific complexes between proteins and helical DNA, *Methods Enzymol* ***208***, 291–343.
29. Chen, X., Agarwal, A., and Giedroc, D.P. (1998) Structural and functional heterogeneity among the zinc fingers of human MRE-binding transcription factor-1, *Biochemistry* ***37***, 11152–11161.
30. Arunkumar, A.I., Campanello, G.C., and Giedroc, D.P. (2009) Solution structure of a paradigm ArsR family zinc sensor in the DNA-bound state, *Proc Natl Acad Sci USA*, ***106***, 18177–18182.
31. Popovych, N., Sun, S., Ebright, R. H., and Kalodimos, C. G. (2006) Dynamically driven protein allostery, *Nat Struct Mol Biol* ***13***, 831–838.